ACS Catalysis

Research Article

pubs.acs.org/acscatalysis

Oxidation of Olefins with Hydrogen Peroxide Catalyzed by Bismuth Salts: A Mechanistic Study

Maxim L. Kuznetsov,*[,†] Bruno G. M. Rocha,[†] Armando J. L. Pombeiro,[†] and Georgiy B. Shul'pin[‡]

[†]Centro de Química Estrutural, Instituto Superior Técnico, Universidade de Lisboa, Avenida Rovisco Pais, 1049-001 Lisbon, Portugal

[‡]Semenov Institute of Chemical Physics, Russian Academy of Sciences, ulitsa Kosygina, dom 4, Moscow 119991, Russia

Supporting Information

ABSTRACT: Theoretical (DFT) calculations predict that soluble Bi salts exhibit catalytic activity toward oxidation of olefins with H_2O_2. Reaction occurs via two competitive channels: (i) nonradical epoxidation of the C=C double bond and (ii) radical hydroperoxidation of the allylic C atom(s) with involvement of the HO• radicals, realized concurrently and leading to epoxide/diol and alkenylhydroperoxide products, respectively. The most plausible mechanism of epoxidation includes the substitution of a water ligand in the initial Bi aqua complex, hydrolysis of the coordinated H_2O_2, one-step oxygen transfer through a direct olefin attack at the unprotonated O atom of the OOH^- ligand in $[Bi(H_2O)_5(OOH)]^{2+}$, and liberation of the epoxide from the coordination sphere of Bi. The main conclusions of the theoretical calculations were confirmed by preliminary experiments on oxidation of cyclohexene, cyclooctene, and 1-octene with the systems $Bi(NO_3)_3/H_2O_2/CH_3CN + H_2O$ and $BiCl_3/H_2O_2/CH_3CN + H_2O$.

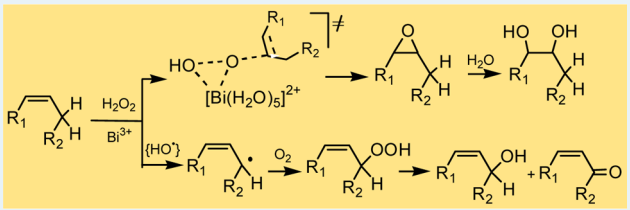

KEYWORDS: *bismuth, DFT calculations, epoxidation, homogeneous catalysis, hydrogen peroxide, olefins, reaction mechanism*

INTRODUCTION

Oxidation of hydrocarbons to valuable products (alcohols, ketones, carboxylic acids, epoxides, etc.) is of tremendous importance and attracts much current attention because of the search for new raw materials for the chemical industry.[1] Hydrogen peroxide is one of the most environmentally benign oxidants used in these processes because water is the only product of H_2O_2 reduction and O_2 is the sole byproduct.[2] The oxidation of hydrocarbons with peroxides usually requires the presence of a catalyst. Transition metal complexes (TMCs) or metal oxides are typically used as such catalysts.[1,3] In contrast, the application of nontransition metal complexes (those of alkaline earth metals, Al, Ga, In, Tl, Sn, Pb, and Bi) in these reactions is much rarer. Most of the publications concern heterogeneous catalysis in which non-TMCs are used as supports[4] or as catalysts themselves.[5−7] Examples of homogeneous oxidations of alkanes or olefins with peroxides catalyzed by non-TMCs include the hydroperoxidation of simple alkanes bearing nonactivated C−H bonds in the presence of $[Al(H_2O)_6]^{3+}$,[8] $[Be(H_2O)_4]^{2+}$, and $[M(H_2O)_6]^{3+}$ (M = Zn, Cd)[9] and epoxidation of olefins with $[Al(H_2O)_6]^{3+}$,[10] Sn(IV) (theoretical study),[11] and Ga(III) (experimental[12] and theoretical[13] studies) species.

Bismuth and its compounds are potentially valuable but clearly underexplored non-TM catalysts in hydrocarbon oxidations.[14] The works on this topic include the oxidation of cyclohexane by molecular oxygen[15] or H_2O_2[16] catalyzed by Bi-containing SBA-15, MCM-41, or ZSM-5 mesoporous molecular sieves; bismuth-catalyzed benzylic or allylic oxidations with *tert*-butyl hydroperoxide;[17] benzylic oxidations by sodium bismuthate $NaBiO_3$ in acetic acid;[18] propylene epoxidation with molecular oxygen catalyzed by a $MoO_3-Bi_2SiO_5/SiO_2$ system;[19] oxidation of propylene or isobutene to acrolein over $Bi_{1-x/3}V_{1-x}Mo_xO_4$[20] and $Bi_xM_yO_z$ (M = Mo, W, Sn)[21] catalysts; and epoxidation of stilbene by ^{t}BuOOH with $[Cp_2Mo(Bi\{OCH(CF_3)_2\}_2)_2]$.[22] The interaction of bismuth oxide clusters with olefins in the presence of O_2 was also studied by theoretical[23] and experimental[24] methods.

Recently,[25] we demonstrated that the simple bismuth nitrate salt $Bi(NO_3)_3$ efficiently catalyzes homogeneous oxidation of alkanes (cyclooctane, *n*-octane, methylcyclohexane, 1,2-dimethylcyclohexane) with H_2O_2 in aqueous CH_3CN. Alkylhydroperoxides formed as a result of this reaction give, upon decomposition, the corresponding alcohols and ketones with a total yield up to 32%, on the basis of the starting alkane. The experimental reaction selectivity parameters indicated that the reaction occurs via a free radical mechanism involving generation of HO• radicals. A plausible mechanism of HO• formation was proposed and theoretically studied. It includes the substitution of a water ligand for H_2O_2 in the aqua complex $[Bi(H_2O)_8]^{3+}$ (this aqua complex is formed upon dissolution of $Bi(NO_3)_3$ in acidified aqueous acetonitrile), hydrolysis of the H_2O_2 adduct, a second H_2O-for-H_2O_2 substitution, and homolytic HO−OH bond cleavage in the intermediate $[Bi(H_2O)_4(H_2O_2)(OOH)]^{2+}$ (Scheme 1). The generated HO• radicals abstract hydrogen from the alkane molecules

Received: January 15, 2015
Revised: April 29, 2015
Published: May 12, 2015

DOI: 10.1021/acscatal.5b00077
ACS Catal. 2015, 5, 3823−3835

Scheme 1. Generation of the HO• Radical in the System $[Bi(H_2O)_8]^{3+}/H_2O_2$

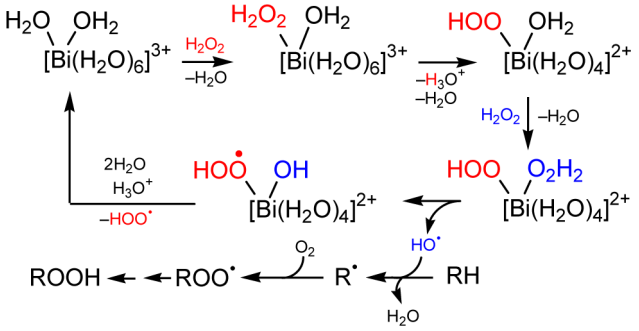

RH to give alkyl radicals R• which, upon fast reaction with molecular oxygen, are transformed into alkylperoxo radicals ROO• and then into alkylhydroperoxide ROOH. The calculated Gibbs free energy of activation for this mechanism is only 15.2 kcal/mol, suggesting that HO• radicals should, indeed, be easily generated in this system. The same mechanism was previously calculated by us also for non-TMCs of group III metals (Al, Ga, In),[26] Be, Zn, and Cd.[9]

When the same catalytic system, $Bi(NO_3)_3/H_2O_2$, is applied for oxidation of olefins instead of alkanes, we can envisage that two competitive processes may occur concurrently: (i) epoxidation/dihydroxylation of the C=C bond via a non-radical mechanism and (ii) hydroperoxidation of the allylic carbon atom via an H-abstraction by a HO• radical to give alkenylhydroperoxide, which is then decomposed to the corresponding alkenol and alkenone (Scheme 2).

Thus, the essential goals of this work are to uncover, by theoretical methods, if the $Bi(NO_3)_3/H_2O_2$ catalytic system is also active toward olefin epoxidation and to elucidate which process, epoxidation or radical hydroperoxidation, is more favorable when olefin is taken as a substrate. Various plausible mechanisms of the epoxidation are compared, details of the most favorable one are discussed, and the main factors determining the catalytic activity are analyzed. To our knowledge, utilization of Bi and its compounds for the homogeneous epoxidation of olefins has not yet been reported.

COMPUTATIONAL DETAILS

The full geometry optimization of all structures and transition states (TS) has been carried out at the DFT/HF hybrid level of theory using Becke's three-parameter hybrid exchange functional in combination with the gradient-corrected correlation functional of Lee, Yang, and Parr (B3LYP)[27] with the help of the Gaussian 09[28] program package. The quasirelativistic Stuttgart pseudopotential that describes 78 core electrons (MWB78) and the appropriate contracted basis set[29] were employed for the Bi atoms. This basis set was augmented by addition of the *f* function with exponent 0.305 optimized using the utility gauopt for the Bi atom in the ground state. The standard basis set 6-311+G(d,p)[30] was applied for all other atoms. No symmetry operations have been applied for any of the structures calculated. Restricted approximations for the structures with closed electron shells and unrestricted methods for the structures with open electron shells have been employed.

Taking into account the importance of the consideration of the second coordination sphere in solvent effect calculations for reactions involving highly charged species, one solvent molecule (H_2O or H_2O_2) was added explicitly in the second shell of the calculated structures. The combination of this model with the B3LYP functional and the basis set used was previously successfully applied for the investigation of hydrocarbon oxidation and epoxidation with H_2O_2 catalyzed by nontransition metal complexes,[9,25,26] providing excellent agreement between the calculated and experimental activation energies of the key reaction steps (see also the Supporting Information for additional discussion concerning the Bi-based species).

The Hessian matrix was calculated analytically for the optimized structures to prove the location of correct minima (no imaginary frequencies) or saddle points (only one imaginary frequency) and to estimate the thermodynamic parameters, the latter being calculated at 25 °C. The nature of all transition states was investigated by the analysis of vectors associated with the imaginary frequency and, in some cases, by the calculations of the intrinsic reaction coordinates (IRC) using the Gonzalez–Schlegel method.[31]

Total energies corrected for solvent effects (E_s) were estimated at the single-point calculations on the basis of gas-phase geometries using the polarizable continuum model in the CPCM version[32] with CH_3CN taken as solvent. The calculations of the solvent effect were carried out using the Gaussian 03[33] program package on the basis of gas-phase equilibrium structures found with Gaussian 09 to provide direct comparison of results obtained in this work and previously.[9,25,26] The UAKS model[34] was applied for the molecular cavity. The entropic term for the CH_3CN solvent (S_s) was calculated according to the procedure described by Wertz and Cooper and Ziegler[35] using eqs 1 − 4

$$\Delta S_1 = R \ln(V^{s}_{m,liq}/V_{m,gas}) \quad (1)$$

$$\Delta S_2 = R \ln(V^{0}_{m,liq}/V^{s}_{m,liq}) \quad (2)$$

$$\alpha = [S^{0,s}_{liq} - (S^{0,s}_{gas} + \Delta S_1)]/[S^{0,s}_{gas} + \Delta S_1] \quad (3)$$

Scheme 2. Oxidation of Cyclohexene Taken as a Model Olefin with the System $Bi(NO_3)_3/H_2O_2$

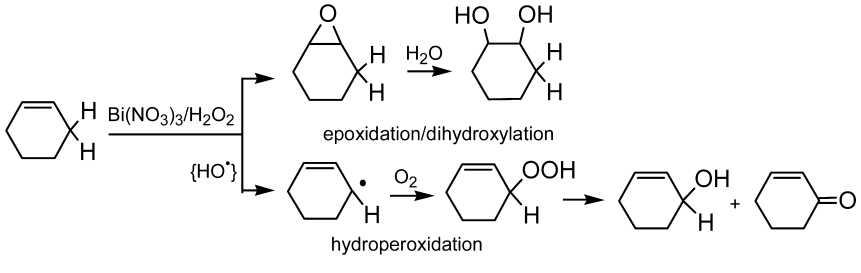

DOI: 10.1021/acscatal.5b00077
ACS Catal. 2015, 5, 3823−3835

$$S_s = S_g + \Delta S_{sol}$$
$$= S_g + [\Delta S_1 + \alpha(S_g + \Delta S_1) + \Delta S_2]$$
$$= S_g + [(-12.21\text{cal/mol·K}) - 0.23(S_g - 12.21\text{cal/mol·K}) + 5.87\text{cal/mol·K}] \quad (4)$$

where S_g = gas-phase entropy of solute, ΔS_{sol} = solvation entropy, $S^{0,s}_{liq}$, $S^{0,s}_{gas}$, and $V^{s}_{m,liq}$ = standard entropies and molar volume of the solvent in liquid or gas phases (149.62 and 245.48 J/mol·K and 52.16 mL/mol, respectively, for CH_3CN), $V_{m,gas}$ = molar volume of the ideal gas at 25 °C (24450 mL/mol), V^0_m = molar volume of the solution corresponding to the standard conditions (1000 mL/mol). The enthalpies and Gibbs free energies in solution (H_s and G_s) were estimated using the expressions $H_s = E_s + H_g - E_g$ and $G_s = H_s - T{\cdot}S_s$, where E_g and H_g are the gas-phase total energy and enthalpy. The relative energies discussed in the text are Gibbs free energies in solution if not stated otherwise.

The topological analysis of the electron density distribution with help of the AIM method of Bader[36] was performed using the program AIMAll.[37] The Wiberg bond indices (B_i)[38] and atomic charges have been computed by using the natural bond orbital (NBO) partitioning scheme.[39] The synchronicity of the Sharpless mechanism (S_y) was calculated using the formula[40]

$$S_y = 1 - (2n-2)^{-1}\cdot\sum_{i=1}^{n}\frac{|\delta B_i - \delta B_{av}|}{\delta B_{av}} \quad (5)$$

where n is the number of bonds directly involved in the reaction. δB_i is the relative variation of a given B_i at the transition state relative to reactants (R) and products (P) and it is calculated as

$$\delta B_i = \frac{B_i^{TS} - B_i^{R}}{B_i^{P} - B_i^{R}} \quad (6)$$

The average value of δB_i (δB_{av}) is defined as

$$\delta B_{av} = n^{-1}\sum_{i=1}^{n}\delta B_i \quad (7)$$

In experimental studies of the hydrocarbon oxidation with H_2O_2 catalyzed by nontransition metal complexes,[8,9] the mixed solvent $CH_3CN + H_2O$ was used. In calculations, the water part of this solvent was approximated by the explicit inclusion of one H_2O molecule in the second coordination shell, whereas the acetonitrile part of the solvent was approximated by the CPCM calculations of the bulky solvent effect for CH_3CN.

EXPERIMENTAL DETAILS

Reagents $Bi(NO_3)_3{\cdot}5H_2O$ (98%), $BiCl_3$ (98%), hydrogen peroxide (50% aqueous solution), cyclohexene (99%), cyclooctene (99%), and 1-octene (98%) were used as received from Sigma-Aldrich. The catalyst was used in the form of a stock solution in acetonitrile. Acetonitrile was selected because other common solvents (e.g., benzene, toluene, $CHCl_3$, CH_2Cl_2, CH_3NO_2, THF, ROH, RC(=O)R′) either directly and actively participate in the oxidation under reaction conditions or form heterogeneous system as a result of insolubility of the catalyst, or they are not miscible with the aqueous H_2O_2. Aliquots of the stock solution were added to the reaction mixtures in the olefin oxidation. The reactions with H_2O_2 (50% aqueous) were typically carried out in air in thermostated Pyrex cylindrical vessels with vigorous stirring, and the total volume of the reaction mixture was 10 mL. (**CAUTION:** the combination of air or molecular oxygen and H_2O_2 with organic compounds at elevated temperatures may be explosive!) The reactions were stopped by cooling and addition of PPh_3 and typically analyzed twice, that is, before and after the addition of an excess of solid PPh_3 using the method developed previously by one of us.[2b,41] For precise determination of oxygenate concentrations, only data obtained after reduction in the reaction sample with PPh_3 were used. Solutions in acetonitrile were analyzed after addition of nitromethane as a standard compound by GC (instrument, HP 5890 Series II; fused-silica capillary column, Hewlett-Packard; the stationary phase was polyethylene glycol INNOWAX with parameters 25 m × 0.2 mm × 0.4 μm; carrier gas was helium with column pressure of 15 psi). Attribution of peaks was made by comparison with chromatograms of authentic samples. A Perkin Elmer Clarus 600 gas chromatograph equipped with two capillary columns (SGE BPX5; 30 m × 0.32 mm × 25 μm), one having EI-MS (electron impact) and the other one with FID detectors, was also used for analyses of the reaction mixtures. Helium was used as the carrier gas (1 mL per minute flow). All EI mass spectra were recorded with 70 eV energy.

RESULTS AND DISCUSSION

Epoxidation Mechanisms. There are two main groups of proposed olefin epoxidation mechanisms: (i) concerted (one-step) oxygen transfer involving one transition state and no intermediates and (ii) stepwise mechanisms including the formation of one or several intermediates. The classical mechanism of the first group (the Sharpless mechanism) is based on the formation of a peroxo complex as an active catalytic species.[42] The olefin molecule then attacks the peroxo ligand, and oxygen transfer occurs in one step via a spiro-type transition state (Scheme 3A). As a variant, this mechanism may include a hydroperoxo complex as an active catalytic species instead of the peroxo one.[11,26a,43] In this case, the oxygen transfer is accompanied by the formation of a hydroxo complex (Scheme 3B). Finally, another modification of the Sharpless

Scheme 3. Principal Concerted Mechanisms of Epoxidation: Sharpless mechanism (A), Modified Sharpless Mechanism (B) and Thiel Mechanism (C)

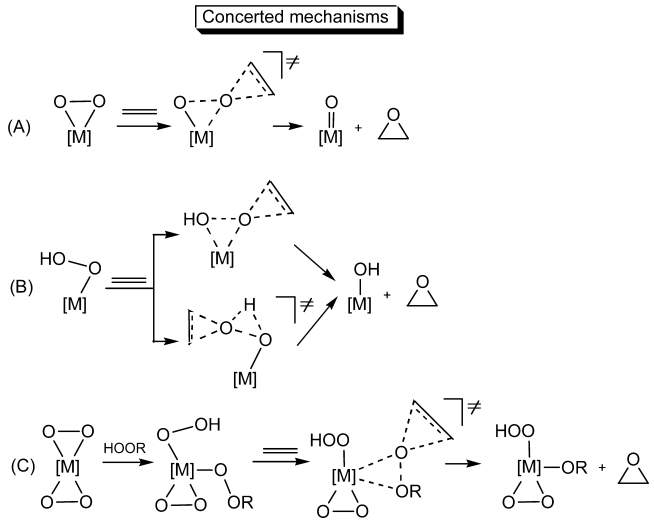

DOI: 10.1021/acscatal.5b00077
ACS Catal. 2015, 5, 3823−3835

Scheme 4. Principal Stepwise Mechanisms of Epoxidation: Mimoun Mechanism (A), Calhorda Mechanism (B) and [2 + 2]-Cycloaddition Mechanism (C)

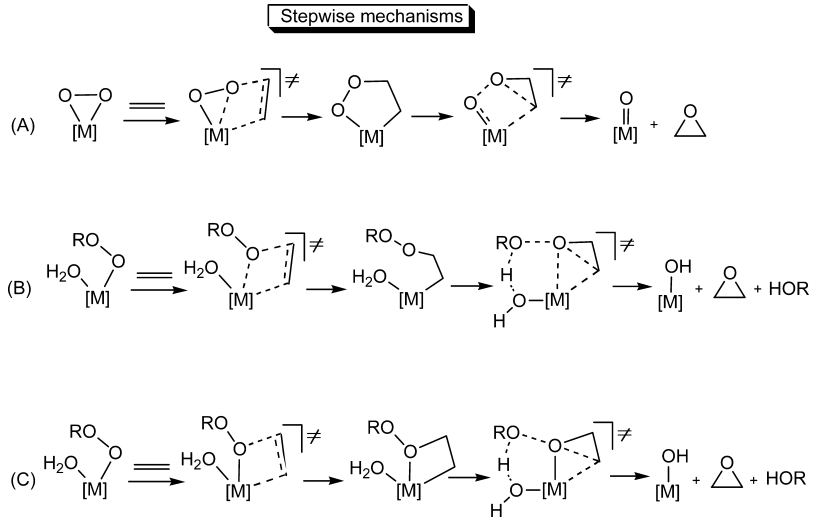

mechanism was proposed by Thiel[44] for the Mo diperoxo catalyst, and it starts with the coordination of a peroxide to the metal and the proton transfer to the peroxo ligand to give the hydroperoxo-alkylperoxo (or dihydroperoxo) complex. One of the hydroperoxo (alkylperoxo) ligands then undergoes the olefin attack and oxygen transfer (Scheme 3C).

The common mechanism of the second group is the Mimoun one.[45] In this pathway, a five-membered metallacyclic intermediate is formed upon insertion of the olefin molecule into an M−O bond of a catalyst. Decomposition of this intermediate leads to the epoxide and the catalyst in the oxo or hydroxo form (Scheme 4A). Another stepwise mechanism was proposed by Calhorda and coauthors.[46] The first step here is also olefin insertion into the M−O bond; however, the intermediate formed is acyclic. The subsequent O−O bond cleavage and intramolecular proton transfer afford the epoxide (Scheme 4B). Finally, the initial step of epoxidation may be the [2 + 2]-cycloaddition of olefin to the M−O bond.[26a] In this mechanism, the intermediate has a four-membered metallacyclic nature (Scheme 4C).

Formation of the Active Catalytic Species. Dissolution of soluble Bi salts [e.g., $Bi(NO_3)_3$] in water in the presence of a strong acid results in the formation of aqua complexes $[Bi(H_2O)_n]^{3+}$.[47] Recently,[25] it was shown by us that the predominant form of the Bi aqua complexes in solution is the octahydrate $[Bi(H_2O)_8]^{3+}$ (**1**). In the same work, the mechanism of formation of the Bi hydroperoxo complex $[Bi(H_2O)_5(OOH)]^{2+}$ (**3**) in the presence of H_2O_2 has also been investigated, and it includes the initial substitution of one water ligand in $[Bi(H_2O)_8]^{3+}$ for H_2O_2 to give $[Bi(H_2O)_7(H_2O_2)]^{3+}$ (**2**). This substitution occurs via a dissociative pathway as shown in Scheme 5, with the low activation barrier of 5.8 kcal/mol reflecting the high lability of the Bi(III) complexes.[48] Because of the highly acidic nature of the hydrated Bi(III) species (pK_a = 1.1),[49] complex **2** then undergoes an easy hydrolysis and a loss of two H_2O molecules, leading to the hydroperoxo complex $[Bi(H_2O)_5(OOH)]^{2+}$ (**3**) (Scheme 5). The calculations demonstrated that **3** is only 3.4 kcal/mol above the initial aqua complex **1** (Figure 1). Thus, the formation of the active catalytic species **3** is highly favorable in terms of kinetic arguments and is not forbidden thermodynamically.

Scheme 5. Mechanism of Formation of $[Bi(H_2O)_5(OOH)]^{2+}$

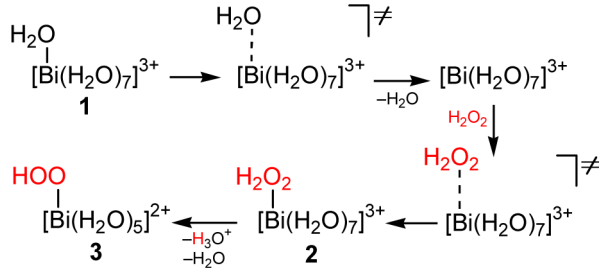

In addition, the calculations revealed that the elimination of one water ligand in **3** may result in the formation of the penta-coordinated complex $[Bi(H_2O)_4(OOH)]^{2+}$ (**4**) with an activation barrier of 7.2 kcal/mol. Despite **4**'s being less stable than **3** by 5.4 kcal/mol, it may also be involved in the epoxidation, and hence, the oxygen transfer mechanisms were considered for both complexes **3** and **4**.

Concerted Mechanisms. *1. Pathways Based on the Hydroperoxo Complexes **3** and **4**; Olefin Attack at the Unprotonated Oxygen Atom.* One transition state of the concerted mechanism corresponding to an attack of the olefin at the coordinated unprotonated oxygen atom of the OOH^- ligand was found for each epoxidation reaction of **3** or **4** (**TS1** and **TS2**, respectively; ethylene was taken as a model of substrate; see Scheme 6). Because the routes based on these TSs were found to be the most favorable ones (see below), a more detailed discussion of this mechanism is provided in the following sections.

(i) Structures of Transition States. The polyhedron of **TS1** is derived from the pentagonal pyramid structure found for the parent complex **3** (Figure 2). However, distortions of the polyhedron in **TS1** from the idealized pyramid are more significant than in **3**. The pentagonal pyramid structural motif is known for Bi(III) complexes, and it reflects a well-known effect of the stereochemically active lone electron pair of Bi. The coordination polyhedron of **TS2** may be better described as a highly distorted trigonal bipyramid (assuming that the OOH^- ligand occupies one coordination place).

DOI: 10.1021/acscatal.5b00077
ACS Catal. 2015, 5, 3823−3835

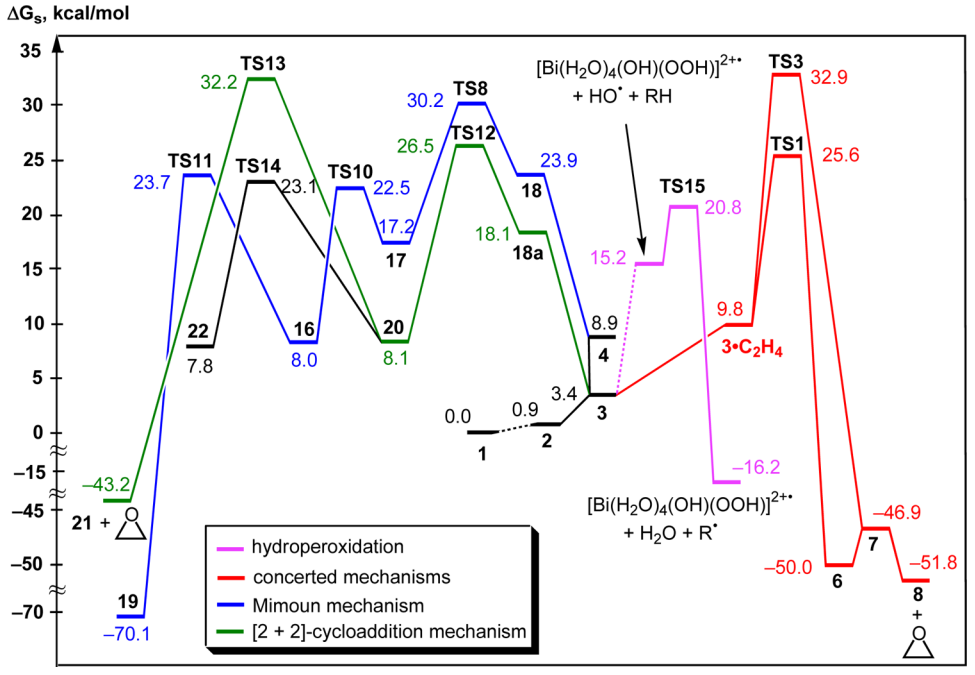

Figure 1. General energy profile for the main proposed mechanisms of epoxidation and hydroperoxidation of olefins (only metal-containing species are indicated, except epoxide and the hydroperoxidation step; second-sphere solvent molecules are omitted; numbers indicate the relative energies).

Scheme 6. Concerted Mechanisms of Epoxidation Based on TS1 and TS2

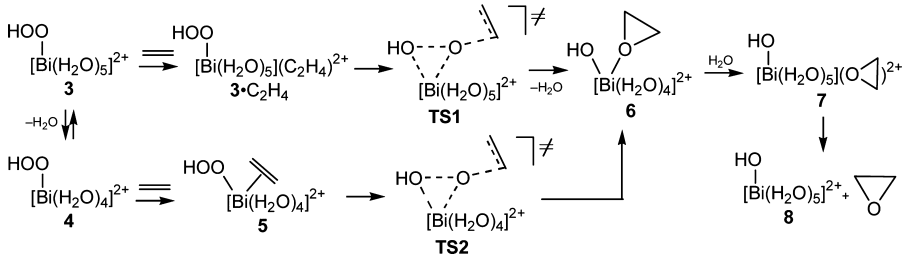

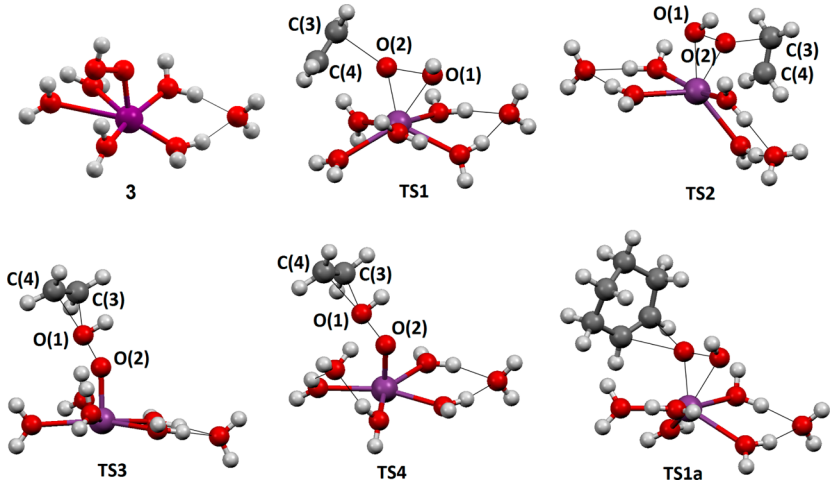

Figure 2. Equilibrium geometries of complex **3** and selected transition states.

The {Bi(OOH)(C_2H_4)} reaction center of these TSs is asymmetric. The Bi−O(1) bond is noticeably longer than Bi−O(2) (2.265/2.260 Å vs 2.130/2.123 Å); however, the OOH^- ligand is in the η^2-coordination mode. One of the C−O bonds is also significantly longer than another one (2.546/2.649 vs 2.285/2.340 Å). The O(1)−O(2) and C(3)−C(4) bonds (1.722/1.670 and 1.348/1.346 Å) are elongated compared with the corresponding bonds in **3**/**4** and in free ethylene (1.464/1.453 and 1.329 Å).

Another interesting structural feature of **TS1** and **TS2** is their significant deviation from the classical spiro-type geometry. Structures with the angle between two connected planes of

DOI: 10.1021/acscatal.5b00077
ACS Catal. 2015, 5, 3823−3835

~90° are typical not only for spiro-compounds with the quaternary carbon atom but also for TSs of the Sharpless mechanism of epoxidation.[51] However, in **TS1**, this angle is significantly lower, ~33°, making the whole geometry of the reaction center more flat. In **TS2**, both BiO(1)O(2) and O(2)C(3)C(4) rings lie almost in the same plane (the angle between the planes is ~6°).

The topological analysis of the electron density distribution (AIM) revealed the existence of bond critical points (BCPs) for five bonds of the reaction center in **TS1** and **TS2** (i.e. BiO(1), BiO(2), O(1)O(2), O(2)−C(3), and C(3)−C(4)), whereas there is no BCP for the O(2)C(4) bond. Thus, these transition states cannot be described as spiro-type structures; instead, the O(2) atom is bound only with one carbon atom of the olefin molecule. The AIM properties at the bond critical points are given in Table S1 in the Supporting Information.

(ii) Intrinsic Reaction Coordinate (IRC). To investigate the mechanism in more detail, the IRC calculations were carried out. The mechanism involving **TS1** starts with the molecular complex between **3** and the ethylene molecule (Scheme 6). The energy of this complex is higher than the sum of energies of isolated **3** and C_2H_4 by 6.4 kcal/mol as a result of unfavorable entropic factor (Figure 1). In contrast, the route via **TS2** includes the formation of the π-complex $[Bi(H_2O)_4(OOH)(C_2H_4)]^{2+}$ (**5**) with Bi−C distances of 3.035 and 3.101 Å.

The evolution of **TS1** or **TS2** leads to the same epoxide adduct $[Bi(H_2O)_4(OH)(OC_2H_4)]^{2+}$ (**6**). The Bi−$O_{epoxide}$ bond length is 2.466 Å in **6**, which is quite comparable with the Bi−O_{water} bond lengths of 2.415−2.523 Å. The epoxide ligand in **6** may undergo a slightly endoergonic substitution by water (ΔG_s = 3.1 kcal/mol) to give the molecular complex $[Bi(H_2O)_5(OH)](OC_2H_4)^{2+}$ (**7**). The substitution of the epoxide in the second coordination sphere of **7** by water releases 5.0 kcal/mol, leading to the separation of $[Bi(H_2O)_5(OH)](H_2O)^{2+}$ (**8**) and OC_2H_4. The variations of the main bond lengths and energy along the reaction coordinate are shown in Figure 3.

(iii) Synchronicity. The concept of synchronicity initially proposed for the concerted cycloaddition reactions[40] may also be used for the concerted mechanisms of olefin epoxidation. There are several criteria of the mechanism synchronicity, and among them are (i) the relative lengths of two newly formed bonds in the transition state, (ii) the relative values of the corresponding Wiberg bond indices, and (iii) the definition of synchronicity (S_y) using eq 5 (see Computational Details). In the last definition, all bonds directly involved in the reaction are considered. The parameter S_y is a quantitative measure showing how synchronously bonds directly involved in a reaction are changed, and it varies from 0 for the stepwise mechanism to 1 for the perfectly concerted one.

Analysis of the first criterion indicates a significant difference between the lengths of two newly forming O−C bonds in TSs (0.261/0.309 Å); however, the difference of the Wiberg bond indices for these bonds is only 0.02, and the S_y parameter is 0.88/0.90 if considering three bonds (C−O and C−C) or 0.90/0.79 if considering six bonds (C−O, Bi−O, C−C, and O−O). Thus, despite the transition states' being rather asymmetric, the oxygen transfer process should be described as rather synchronous. This is also confirmed by the synchronous change of the O−C, Bi−O, O−O, and C−C bond lengths along the reaction path (Figure 3).

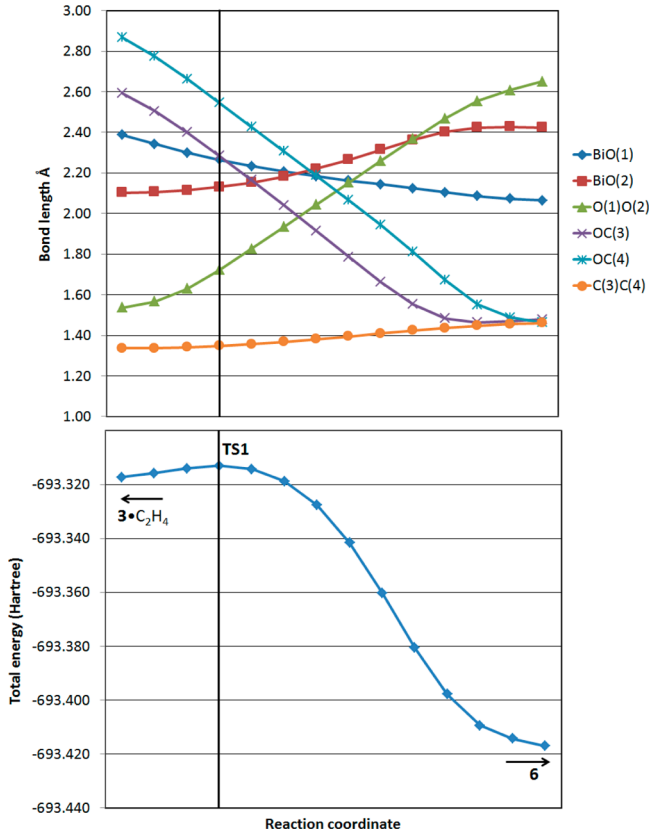

Figure 3. Intrinsic reaction coordinate and change of selected internuclear distances along the reaction path for the mechanism based on **TS1**. For the atomic numbering, see Figure 2.

(iv) Electron Transfer. In terms of the electron transfer, a concerted epoxidation may be described either as a nucleophilic addition of olefin to the hydroperoxo ligand or as a nucleophilic attack of the hydroperoxo ligand at the olefin molecule. In the former case, the reaction is controlled by the $HOMO_{olefin}$−$LUMO_{OOH}$ type of the FMO interactions, whereas in the latter case, the $HOMO_{OOH}$−$LUMO_{olefin}$ interaction is predominant. The FMOs of complexes **3** and **4** with an appropriate symmetry that can interact with MOs of olefin are HOMO ($\pi^*_{\perp O-OH}$) and LUMO+4 (σ^*_{O-OH}) (Figure 4). The $HOMO_{3/4}$−$LUMO_{C_2H_4}$ gap is 14.4 eV, whereas the $HOMO_{C_2H_4}$−$LUMO{+}4_{3/4}$ gap is only 0.7−0.9 eV. These values indicate unambiguously that the reaction between **3**/**4** and olefin represents a nucleophilic addition of C_2H_4 to the peroxo ligand of the Bi complexes.

This conclusion is confirmed by the natural bond orbital (NBO) analysis. The total NBO charge at the C_2H_4 fragment in **TS1** and **TS2** is significantly positive (0.21−0.26 e), demonstrating the release of the charge density from ethylene upon formation of TSs. The total second-order perturbation energy for the **3**/**4** → C_2H_4 charge transfer in **TS1**/**TS2** is 8.1/6.2 kcal/mol, the highest contribution being from the n[O(2)] → $\pi^*(C_2H_4)$ transition (2.5/2.9 kcal/mol). At the same time, the overall $E(2)$ energy for the C_2H_4 → **3**/**4** charge transfer is 41.6/33.5 kcal/mol, with the highest contribution coming from the $\pi(C_2H_4)$ → π^*(O−O) transition (31.3/22.4 kcal/mol).

*2. Pathways Based on the Hydroperoxo Complexes **3** and **4**; Olefin Attack at the Protonated Oxygen Atom.* The approaching olefin molecule can also attack the other oxygen atom of the OOH^- ligand, that is, the protonated one (Scheme

DOI: 10.1021/acscatal.5b00077
ACS Catal. 2015, 5, 3823−3835

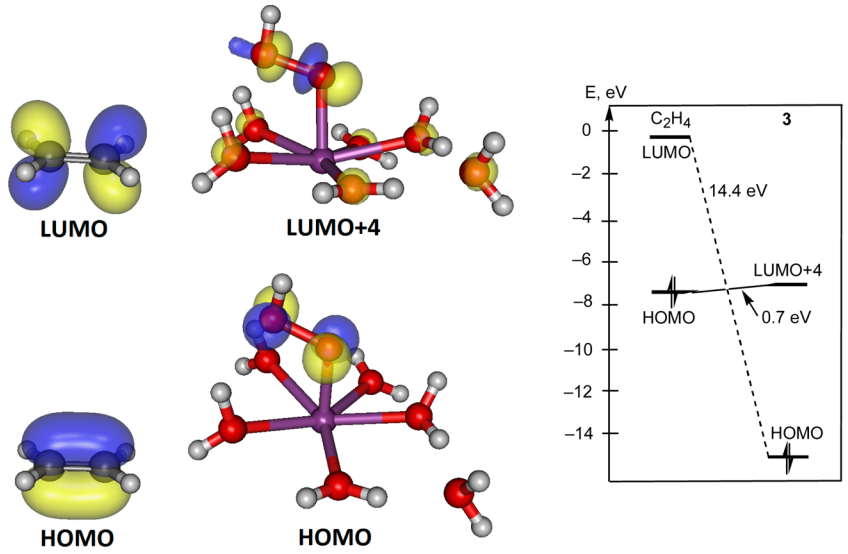

Figure 4. Plots of the interacting molecular orbitals of C_2H_4 and **3** and their relative energies.

Scheme 7. Concerted Mechanisms of Epoxidation Based on TS3 and TS4

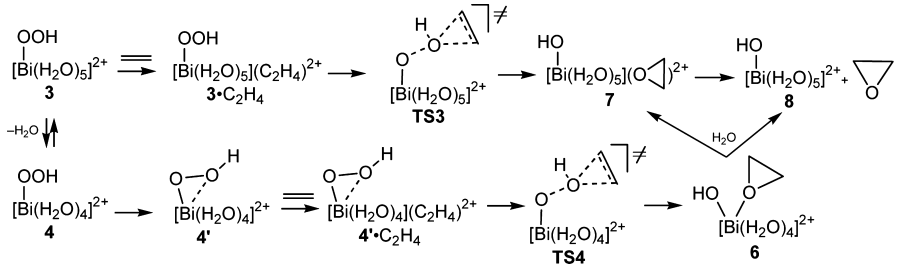

Scheme 8. Sharpless Mechanism of Epoxidation

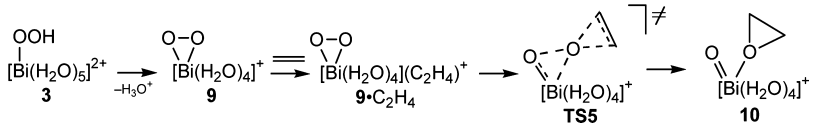

7). The transition state of this pathway was located for each complex **3** and **4** (**TS3** and **TS4**, respectively). The coordination polyhedra of **TS3** and **TS4** are distorted pentagonal and square pyramids, respectively, with the reacting OOH^- ligand situating at the axial position (Figure 2). The latter structural motif is also known for Bi(III) species.[50a,52]

The OOH^- ligand is clearly monodentate, with the BiO(1) and BiO(2) distances of 2.904/3.366 and 2.007/2.009 Å, respectively. The O(1)O(2) bond is significantly dissociated (to 1.829/1.854 Å). The O(1)C(3) and O(1)C(4) bonds are also not equivalent (2.300/2.309 and 2.061/2.144 Å). The AIM analysis showed BCPs for five BiO(2), O(1)O(2), O(1)C(3), O(1)C(4), and C(3)C(4) bonds and one RCP for the OCC ring. Thus, the $\{OO(H)CH_2CH_2\}$ reaction fragment in **TS3** and **TS4** is T-shaped rather than of the spiro type.

The pathway involving **TS3** starts with the formation of the molecular complex $[Bi(H_2O)_5(OOH)](C_2H_4)^{2+}$, which is converted to **TS3** and then directly to the molecular complex $[Bi(H_2O)_5(OH)](OC_2H_4)^{2+}$ **7** without formation of any epoxide adduct with OC_2H_4 ligated to Bi.

In contrast, the pathway through **TS4** begins with a change of the coordination mode of the OOH^- ligand in **4** from the η^1 to the η^2 type (**4** → **4′**). The Bi−O(H) bond length is 2.557 Å in **4′**; such an isomerization is only slightly exoergonic by 0.3 kcal/mol. The molecular complex between **4′** and C_2H_4 is then formed. Transition state **TS4** is converted to the epoxide adduct $[Bi(H_2O)_4(OH)(OC_2H_4)]^{2+}$ **6**, and this process is accompanied by the proton transfer to the Bi-bound oxygen atom.

The calculated S_y parameters for these pathways are 0.86/0.87 if considering three bonds (C−O and C−C) or 0.88/0.89 if considering four bonds (C−O, C−C, and O−O), indicating a rather synchronous character of these processes.

3. Pathway Based on the Peroxo Complex $[Bi(H_2O)_5(OO)]^+$. This classical Sharpless mechanism includes the consecutive formation of the peroxo complex $[Bi(H_2O)_4(OO)]^+$ (**9**) upon hydrolysis of $[Bi(H_2O)_5(OOH)]^{2+}$ (**3**) (no minimum was found for the hexa-coordinated species $[Bi(H_2O)_5(OO)]^+$), a molecular complex between **9** and C_2H_4, with olefin being in the second coordination sphere and then the spiro-type transition state **TS5** (Scheme 8). This TS is converted to the oxo-epoxido complex $[Bi(H_2O)_4(=O)(OC_2H_4)]^+$ (**10**).

4. Pathways Based on the Dihydroperoxo Complex $[Bi(H_2O)_4(OOH)_2]^+$. This Thiel-type mechanism involves the formation of the dihydroperoxo complex $[Bi(H_2O)_4(OOH)_2]^+$

DOI: 10.1021/acscatal.5b00077
ACS Catal. 2015, 5, 3823−3835

Scheme 9. Thiel Mechanism of Epoxidation

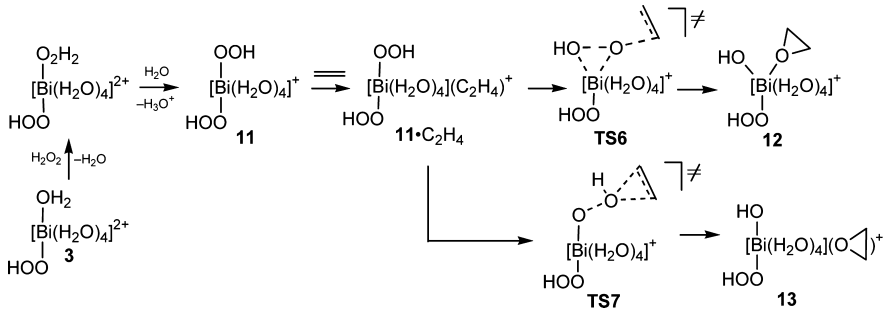

Table 1. Calculated Gibbs Free Energies of Activation ($\Delta G_s^{\neq}$) and Reaction (ΔG_s) in CH_3CN Solution (in kcal/mol)

reaction		$\Delta G_s^{\ddagger}$	ΔG_s
$[Bi(H_2O)_8](H_2O_2)^{3+}$ (**1**) → $[Bi(H_2O)_7(H_2O_2)](H_2O)^{3+}$ (**2**)		5.8	0.8
$[Bi(H_2O)_7(H_2O_2)](H_2O)^{3+}$ (**2**) → $[Bi(H_2O)_5(OOH)](H_2O)^{2+}$ (**3**) + H_3O^+ + H_2O			2.6
$[Bi(H_2O)_5(OOH)](H_2O)^{2+}$ (**3**) → $[Bi(H_2O)_4(OOH)](H_2O)_2^{2+}$ (**4**)		7.2	5.4
$[Bi(H_2O)_5(OOH)](H_2O)^{2+}$ (**3**) + C_2H_4 → $[Bi(H_2O)_5(OOH)](H_2O)(C_2H_4)^{2+}$ (**3**·C_2H_4)			6.4
$[Bi(H_2O)_5(OOH)](H_2O)(C_2H_4)^{2+}$ (**3**·C_2H_4) → $[Bi(H_2O)_4(OH)(OC_2H_4)](H_2O)_2^{2+}$ (**6**)	via **TS1**	15.8	−59.9
$[Bi(H_2O)_4(OH)(OC_2H_4)](H_2O)_2^{2+}$ (**6**) → $[Bi(H_2O)_5(OH)](H_2O)(OC_2H_4)^{2+}$ (**7**)			3.1
$[Bi(H_2O)_5(OH)](H_2O)(OC_2H_4)^{2+}$ (**7**) + H_2O → $[Bi(H_2O)_5(OH)](H_2O)_2^{2+}$ (**8**) + OC_2H_4			−5.0
$[Bi(H_2O)_4(OOH)](H_2O)_2^{2+}$ (**4**) + C_2H_4 → $[Bi(H_2O)_4(OOH)(C_2H_4)](H_2O)_2^{2+}$ (**5**)			6.3
$[Bi(H_2O)_4(OOH)(C_2H_4)](H_2O)_2^{2+}$ (**5**) → $[Bi(H_2O)_4(OH)(OC_2H_4)](H_2O)_2^{2+}$ (**6**)	via **TS2**	11.5	−65.2
$[Bi(H_2O)_5(OOH)](H_2O)(C_2H_4)^{2+}$ (**3**·C_2H_4) → $[Bi(H_2O)_5(OH)](H_2O)(OC_2H_4)^{2+}$ (**7**)	via **TS3**	23.0	−56.7
$[Bi(H_2O)_4(OOH)](H_2O)_2^{2+}$ (**4**) → $[Bi(H_2O)_4(\eta^2\text{-}OOH)](H_2O)_2^{2+}$ (**4′**)			−0.3
$[Bi(H_2O)_4(\eta^2\text{-}OOH)](H_2O)_2^{2+}$ (**4′**) + C_2H_4 → $[Bi(H_2O)_4(\eta^2\text{-}OOH)](H_2O)_2(C_2H_4)^{2+}$ (**4′**·C_2H_4)			6.1
$[Bi(H_2O)_4(\eta^2\text{-}OOH)](H_2O)_2(C_2H_4)^{2+}$ (**4′**·C_2H_4) → $[Bi(H_2O)_4(OH)(OC_2H_4)](H_2O)_2^{2+}$ (**6**)	via **TS4**	18.4	−64.7
$[Bi(H_2O)_4(OO)](H_2O)_2^{+}$ (**9**) + C_2H_4 → $[Bi(H_2O)_4(OO)](H_2O)_2(C_2H_4)^{+}$ (**9**·C_2H_4)			6.1
$[Bi(H_2O)_4(OO)](H_2O)_2(C_2H_4)^{+}$ (**9**·C_2H_4) → $[Bi(H_2O)_4(=O)(OC_2H_4)](H_2O)_2^{+}$ (**10**)	via **TS5**	16.4	−42.5
$[Bi(H_2O)_4(OOH)_2](H_2O)^{+}$ (**11**) + C_2H_4 → $[Bi(H_2O)_4(OOH)_2](H_2O)(C_2H_4)^{+}$ (**11**·C_2H_4)			2.4
$[Bi(H_2O)_4(OOH)_2](H_2O)(C_2H_4)^{+}$ (**11**·C_2H_4) → $[Bi(H_2O)_4(OH)(OOH)(OC_2H_4)](H_2O)^{+}$ (**12**)	via **TS6**	21.3	−44.9
$[Bi(H_2O)_4(OOH)_2](H_2O)(C_2H_4)^{+}$ (**11**·C_2H_4) → $[Bi(H_2O)_4(OH)(OOH)](H_2O)(OC_2H_4)^{+}$ (**13**)	via **TS7**	29.0	−48.5
$[Bi(H_2O)_4(OOH)](H_2O)_2^{2+}$ (**4**) + C_2H_4 → $[Bi(H_2O)_3(OOH)(C_2H_4)](H_2O)_2^{2+}$ (**18**) + H_2O			15.1
$[Bi(H_2O)_3(OOH)(C_2H_4)](H_2O)_2^{2+}$ (**18**) → $[Bi(H_2O)_3\{\underline{O}O(H)CH_2\underline{C}H_2\}](H_2O)_2^{2+}$ (**17**)	via **TS8**	6.2	−6.7
$[Bi(H_2O)_3\{\underline{O}O(H)CH_2\underline{C}H_2\}](H_2O)_2^{2+}$ (**17**) → $[Bi(H_2O)_4\{\underline{O}O(H)CH_2\underline{C}H_2\}](H_2O)^{2+}$ (**15**)			3.1
$[Bi(H_2O)_3\{\underline{O}O(H)CH_2\underline{C}H_2\}](H_2O)_2^{2+}$ (**17**) → $[Bi(H_2O)_3\{\underline{O}(H)OCH_2\underline{C}H_2\}](H_2O)_2^{2+}$ (**16**)	via **TS9**	27.9	−9.2
	via **TS10**	5.3	−9.2
$[Bi(H_2O)_3\{\underline{O}(H)OCH_2\underline{C}H_2\}](H_2O)_2^{2+}$ (**16**) → $[Bi(H_2O)_4\{\underline{O}(H)OCH_2\underline{C}H_2\}](H_2O)^{2+}$ (**14**)			−4.3
$[Bi(H_2O)_3\{\underline{O}(H)OCH_2\underline{C}H_2\}](H_2O)_2^{2+}$ (**16**) → $[Bi(H_2O)_3(OH)(OCHCH_3)](H_2O)_2^{2+}$ (**19**)	via **TS11**	15.6	−78.1
$[Bi(H_2O)_5(OOH)](H_2O)^{2+}$ (**3**) + C_2H_4 → $[Bi(H_2O)_4(OOH)(C_2H_4)](H_2O)^{2+}$ (**18a**) + H_2O			14.7
$[Bi(H_2O)_4(OOH)(C_2H_4)](H_2O)^{2+}$ (**18a**) → $[Bi(H_2O)_4\{\underline{O}(OH)CH_2\underline{C}H_2\}](H_2O)^{2+}$ (**20**)	via **TS12**	8.4	−10.0
$[Bi(H_2O)_4\{\underline{O}(OH)CH_2\underline{C}H_2\}](H_2O)^{2+}$ (**20**) → $[Bi(H_2O)_3(OH)(OCH_2CH_2)](H_2O)_2^{2+}$ (**21**)	via **TS13**	24.1	−51.3
$[Bi(H_2O)_4\{\underline{O}(OH)CH_2\underline{C}H_2\}](H_2O)^{2+}$ (**20**) → $[Bi(H_2O)_4(\underline{C}H_2CH_2OOH)](H_2O)^{2+}$ (**22**)	via **TS14**	15.0	−0.3

(**11**) as a result of water substitution for H_2O_2 in $[Bi(H_2O)_5(OOH)]^{2+}$ (**3**), followed by hydrolysis of the coordinated hydrogen peroxide (Scheme 9). Two pathways are possible then: those via **TS6** corresponding to the olefin attack at the unprotonated O atom of the OOH^- ligand and via **TS7** associated with the attack at the protonated oxygen atom. The first pathways lead to the epoxido adduct $[Bi(H_2O)_4(OH)(OOH)(OC_2H_4)]^+$ (**12**), whereas the second route affords complex $[Bi(H_2O)_4(OH)(OOH)](OC_2H_4)^+$ (**13**), with the epoxide situated in the second coordination sphere.

5. Activation Energies of the Concerted Mechanisms. In gas phase, all four TSs based on the hydroperoxo complexes **3** and **4** (**TS1**−**TS4**) have similar stabilities with the differences within 3 kcal/mol in terms of Gibbs free energies. The stability decreases along the row **TS2** > **TS3** > **TS1** ∼ **TS4**; however, consideration of the solvent effects makes **TS1** and **TS2** clearly more stable than **TS3** and **TS4** (by 6.2−7.4 kcal/mol). In solution, the stability of TSs decreases along the sequence **TS1** > **TS2** > **TS3** ∼ **TS4**, and the activation barriers ($\Delta G_s^{\ddagger}$) of the reaction **3** (→ **4**) + C_2H_4 for these channels are 22.2−29.6 kcal/mol (Table 1).

The activation barriers of the oxygen transfer steps based on **TS5** and **TS6** of the Sharpless and Thiel type mechanisms are similar (22.6 and 23.7 kcal/mol for the reactions **9** + C_2H_4 and **11** + C_2H_4, respectively), whereas the mechanism via **TS7** is clearly less favorable ($\Delta G_s^{\ddagger}$ = 31.4 kcal/mol). At the same time, the formation of both **9** and **11** upon hydrolysis is endoergonic.[53] As a result, the activation barrier of the pathways based on **TS5** and **TS6** relative to **3** should be obviously higher than that for the route via **TS1**. Thus, the pathway based on the monohydroperoxo complex **3** and **TS1** is the most favorable one among all the concerted mechanisms.

The overall lowest activation energy of the concerted epoxidation *relative to the initial complex* ***1*** is 25.6 kcal/mol

DOI: 10.1021/acscatal.5b00077
ACS Catal. 2015, 5, 3823−3835

Scheme 10. Mimoun Mechanism of Epoxidation

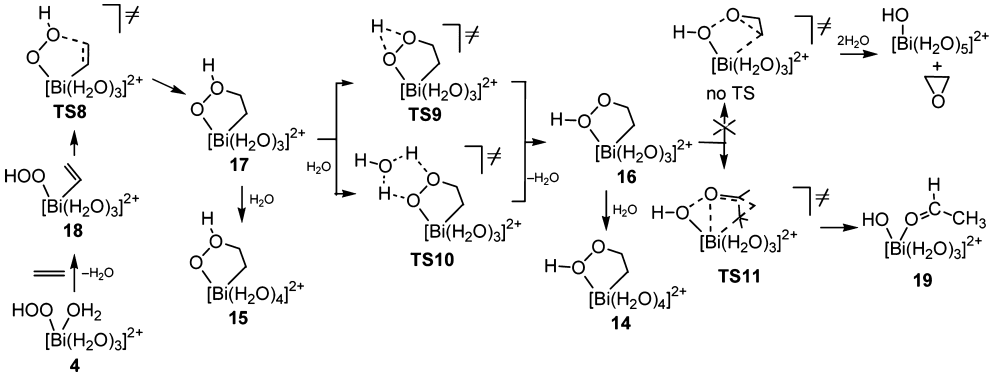

Scheme 11. [2 + 2]-Cycloaddition Mechanism

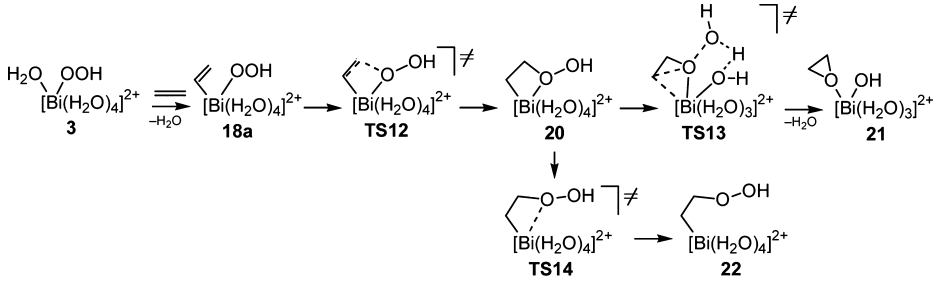

(Figure 1). This value is lower than $\Delta G_s^{\ddagger}$ of the epoxidation with the Al aqua complex $[Al(H_2O)_6]^{3+}$ (28.1 kcal/mol).[26a] Taking into account that the latter complex was found to be active in the epoxidation of *α,β*-unsaturated ketones,[10] the Bi system might also be efficient as a catalyst for this process if the concurrent radical pathway is not operating (see the Introduction).

Stepwise Mechanisms. *1. Mimoun-Type Pathways.* A mechanism of this type was also searched for both starting complexes **3** and **4**. Two types of five-membered metallacyclic intermediates with different protonated oxygen atoms were found for each reaction channel (**14**, **15** and **16**, **17**) (Scheme 10). The intermediates **14** and **16** with the protonated Bi-bound oxygen atom are more stable than **15** and **17** by 16.6 and 9.2 kcal/mol; however, we were unable to locate any transition state for the formation of **14**/**16** from **3**/**4** + C_2H_4, and all attempts led either to an intermediate or to a transition state of another mechanism described in the next section. Similarly, no TS of the formation of the hexa-coordinated intermediate **15** was found. Instead, transition state **TS8** with penta-coordinated Bi atom was located, and this TS leads to **17**.

In agreement with the IRC calculations from **TS8** and subsequent geometry optimization, this mechanism starts with complex $[Bi(H_2O)_3(OOH)(C_2H_4)]^{2+}$ (**18**) as a result of a water substitution for the olefin molecule in **4** (Scheme 10). The AIM analysis shows the presence of one Bi−C bond critical point with the ρ, $\nabla^2\rho$, and H_b values of 0.174 e/Å^3, 0.552 e/Å^5, and −0.018 hartree/Å^3, respectively. These values indicate that the bonding between the Bi and C atoms is rather weak. No BCP between Bi and another C atom, as well as no ring critical point for the Bi−CC cycle, were found. Thus, **18** should be considered as an acyclic species. The AIM data correlate with the long and not equal Bi−C distances in **18** (2.904 and 3.112 Å).

The absence of the corresponding TSs shows that complexes **14**, **15**, and **16** conceivably are not achievable directly upon reaction of the olefin with the hydroperoxo species. However, these intermediates may be formed as a result of a 1,2-hydrogen shift (**17** → **16**) or through a migration of a water molecule from the second coordination sphere to the first one (**16** → **14** and **17** → **15**) (Scheme 10). The hydrogen shift from **17** to **16** may be either direct, via **TS9**, or assisted by a water molecule, via **TS10**. The former process requires a rather high activation barrier of 27.9 kcal/mol, whereas the activation energy of the latter process is much lower (5.3 kcal/mol) as a result of the presence of the 5-membered cyclic fragment O···H···O···H···O in **TS10**.

The final step of the Mimoun-type mechanism is the transformation of the five-membered intermediate to complex $[Bi(H_2O)_n(OH)]^{2+}$ and epoxide. However, no TS for this process was found. Instead, the transition state **TS11** was located with an energy of 15.6 kcal/mol above **16**. Meanwhile, the IRC calculations indicated that this TS corresponds to the formation of the coordinated acetaldehyde CH_3CHO (**19**) instead of ethylene epoxide. A similar situation was found previously for the epoxidations of molybdenum and vanadium peroxo complexes.[51,54]

The calculated activation energies $\Delta G_s^{\ddagger}$ for the formation of intermediate **17** are 26.7 and 30.2 kcal/mol relative to **3** and **1**, respectively. Thus, the realization of the Mimoun-type mechanism is not feasible because (i) it clearly requires a higher activation barrier than the concerted oxygen transfer, and (ii) it leads to the formation of aldehyde instead of epoxide product.

2. [2 + 2]-Cycloaddition and Calhorda-Type Mechanisms. The alternative stepwise mechanism of epoxidation (Scheme 11) is based on the [2 + 2]-cycloaddition of the olefin to the Bi−OOH bond without cleavage of the latter. As a result, the four-membered cyclic intermediate **19** is formed. This

DOI: 10.1021/acscatal.5b00077
ACS Catal. 2015, 5, 3823−3835

Table 2. Maximum Yields (%) of the Oxygenate Products

		yield					
catalyst	substrate	epoxide	enone	enol	*trans* diol	*cis* diol	total
$Bi(NO_3)_3$	cyclohexene	traces	1	12	3	traces	16
$BiCl_3$	cyclohexene	1	traces	13	2		16
$Bi(NO_3)_3$	cyclooctene	14		5	4	1	24
$Bi(NO_3)_3$	1-octene	traces		2	4		6

mechanism starts with the substitution of one water ligand for the olefin molecule in **3** to give the acyclic complex **18a** (BCP for only one Bi−C bond was located using the AIM analysis). Intermediate **20** is formed from **18a** via **TS12**, and then it transforms into the epoxide adduct **21** via **TS13**. The second step of this mechanism is the rate-limiting one; the calculated activation energies are 28.8 and 32.2 kcal/mol relative to **3** and **1**, respectively, which are slightly higher than those for the Mimoun-type mechanism (Figure 1).

A similar mechanism was proposed by Calhorda and coauthors,[46] but it includes the formation of an acyclic intermediate as a result of the [2 + 2] insertion of the olefin molecule into the M−O bond (Scheme 4B). Such intermediate **22** was, indeed, found for the Bi system under study (Scheme 11); however, no TSs associated either with one-step [2 + 2] insertion **3**/**4** + C_2H_4 leading to **22** or with its transformation to epoxide were located. All attempts led either to **TS12** or to **TS13** of the [2 + 2] cycloaddition mechanism. Instead, **TS14** was found, and it corresponds to the Bi−O bond cleavage in **20**. Thus, the acyclic Calhorda-type intermediate is a side product, and it does not belong to the reaction path of the epoxidation process.

In summary, the calculations indicate that among all the considered mechanisms of the epoxidation, the most favorable one is the concerted oxygen transfer from the hydroperoxo ligand in complex $[Bi(H_2O)_5(OOH)]^{2+}$ **3** via **TS1**, with the overall $\Delta G_s^{\ddagger}$ value of 25.6 kcal/mol.

Substrate Nature. The calculations discussed above were carried out for ethylene as the simplest model of olefins. To check how the nature of the substrate affects the activation energy of epoxidation, the calculations with cyclohexene and cyclooctene—olefins often used in experimental works on this topic—were also performed. As a result, the transition states **TS1a** and **TS1b** of the most plausible mechanism were found (Figure 2). The activation barrier, $\Delta G_s^{\ddagger}$, of the reaction with cyclohexene is the same as with ethylene (i.e., 22.2 and 25.6 kcal/mol relative to **3** and **1**, respectively) whereas that of the reaction with cyclooctene is lower by 1.3 kcal/mol. This difference corresponds to the ratio of the reaction rates of the cyclohexene and cyclooctene epoxidation: 1:9.

Comparison of the Nonradical Epoxidation and the Radical Hydroperoxidation Channels. The calculations indicated that the epoxidation of olefins with H_2O_2 catalyzed by soluble Bi salts has an activation barrier sufficiently low to permit the effective realization of this process. However, as was mentioned in the Introduction, another concurrent process in this system is also possible: hydroperoxidation of the allylic carbon atom of the olefin with involvement of the HO$^{\bullet}$ radical (Schemes 1 and 2). The calculated activation barrier of the HO$^{\bullet}$ radical generation in the system $[Bi(H_2O)_8]^{3+}/H_2O_2$ is 15.2 kcal/mol.[25] The HO$^{\bullet}$ radical then abstracts the hydrogen atom from the olefin molecule, affording the R$^{\bullet}$ radical. The calculated activation energy for the reaction HO$^{\bullet}$ + RH → H_2O + R$^{\bullet}$ (R = 2-cyclohexenyl, via **TS15**) is 5.6 kcal/mol. Thus, the overall activation barrier of the cyclohexene hydroperoxidation via the radical mechanism is 20.8 kcal/mol relative to **1**. This value is lower than the activation energy of the nonradical epoxidation (25.6 kcal/mol) (Figure 1). Hence, the calculations predict that the predominant channel of the cyclohexene oxidation with H_2O_2 catalyzed by soluble Bi salts should be hydroperoxidation. At the same time, the difference of the activation barriers for these two channels is not significant, and hence, the formation of epoxide (or products of its hydrolysis) is also quite possible.

Oxidation of Olefins with the $Bi(NO_3)_3/H_2O_2$ and $BiCl_3/H_2O_2$ Systems. To verify the theoretical predictions, a preliminary experimental study of the cyclohexene, cyclooctene, and 1-octene oxidation by H_2O_2 catalyzed by $Bi(NO_3)_3$ and $BiCl_3$ under air atmosphere in aqueous acetonitrile was carried out. The catalyst was introduced in the form of nitrate $Bi(NO_3)_3{\cdot}5H_2O$ or chloride $BiCl_3$. Initial concentrations of substrate, catalyst, and H_2O_2 were 0.25, 1×10^{-3}, and 1.2 M, respectively; temperature, 60 °C; reaction time, up to 32 h. Concentrations of products and yields were typically measured after addition of PPh_3 to the reaction sample.

For the reactions with cyclohexene, the experiments indicate that the total yield of the oxygenate products under these conditions reaches 16%, on the basis of the initial cyclohexene (the overall concentration of the products was 0.041 M after 32 h; see Figures S1, S2 in the Supporting Information). In the absence of the Bi salt, the yield is <2%. The principal product detected by GC after reduction with PPh_3 was 2-cyclohexene-1-ol (yield 12−13%; Table 2) formed via the radical mechanism upon the decomposition of ROOH (Scheme 2). Indeed, the comparison of chromatograms obtained for the reaction samples before and after addition of PPh_3 (Figure S1) demonstrated the formation of cyclohexenyl hydroperoxide, ROOH, during the course of the reaction (for this method, see refs 2b, 41.). At the same time, *trans*-cyclohexane-1,2-diol was also detected as a minor product with a yield of ∼3%. Other possible products of the epoxidation or hydroperoxidation (cyclohexene oxide, *cis*-cyclohexane-1,2-diol, 2-cyclohexene-1-one) were formed in trace amounts. The formation of *trans*-cyclohexane-1,2-diol instead of cyclohexene oxide was quite expected, considering that epoxides are easily hydrolyzed under acidic conditions at elevated temperatures (note that the soluble Bi^{3+} salts are strong acids with a pK_a value of 1.1,[49] and the reaction temperature was 60 °C). The well-known S_N2 mechanism of this hydrolysis shown in Scheme 12 explains the exclusive formation of the *trans* isomer of the diol.

Scheme 12. Hydrolysis of Cyclohexene Oxide

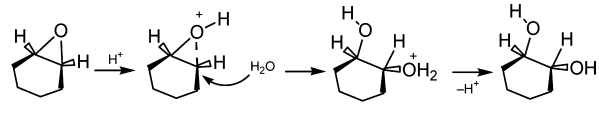

DOI: 10.1021/acscatal.5b00077
ACS Catal. 2015, 5, 3823−3835

The initial reaction rate, W_0, was determined from the slope of the tangent to the kinetic curves of the corresponding oxygenate accumulation after addition of PPh_3 to the reaction mixture (Figure S1). The initial reaction rate of the accumulation of enol (the principal final product of the hydroperoxydation pathway) (6.1×10^{-7} M/s) is ~3 times higher than the W_0 value of the formation of *trans* diol (the main product of the epoxidation pathway) (2.2×10^{-7} M/s), and the selectivity parameter for these two products after 32 h is enol/*trans*-diol = 4:1. At the same time, it is necessary to mention that in the case of the hydroperoxidation pathway, a number of side reactions are possible; for example, interaction of the highly reactive $HO^{\bullet}$ radicals with other components of the system, such as solvent, ROOH, H_2O_2, $HOO^{\bullet}$, intermediates formed in the course of the reaction, or with impurities that inevitably exist in the reaction mixture or are adsorbed on walls. All these side reactions provide a low selectivity of the radical pathway and decrease the accumulation rate of the enol product, despite the efficient $HO^{\bullet}$ radical generation predicted by the DFT calculations. However, even despite such an effect of the $HO^{\bullet}$ radicals' consumption in side reactions, enol still appears as a major product.

The total yield of the oxygenates in the reaction with cyclooctene reaches 24% after 24 h, and the main product is cyclooctene oxide (14%), whereas 2-cyclooctene-1-ol and *trans*-cyclooctane-1,2-diol were obtained in yields of 5 and 4%, respectively (Table 2, Figure S3). The preferential formation of epoxide is accounted for by the known higher thermodynamic stability of cyclooctene oxide. The increase in yields of the epoxidation products relative to those of the hydroperoxidation pathway in this case is in agreement with the results of the theoretical studies indicating that the activation barrier of the cyclooctene epoxidation is lower than that of the cyclohexene epoxidation (see above, Substrate Nature section).

The total yield of the 1-octene oxidation products is lower and reaches 6%; the principal product is octane-1,2-diol (4%), whereas the yield of 1-octene-3-ol is ~2% (Table 2, Figure S4). The low yield of the enol product may be accounted for by (i) the lower number of the allylic hydrogen atoms in 1-octene (two atoms) compared with the cyclic olefins (four atoms) and (ii) the less reactive C−H allylic bond in 1-octene. The latter is confirmed by the DFT calculations, indicating that the activation energy of the allylic hydrogen abstraction by $HO^{\bullet}$ from 1-octene is 6.8 kcal/mol vs 5.6 kcal/mol for cyclohexene. Such a difference corresponds to the lower reactivity of 1-octene toward hydroperoxidation by a factor of 8, in agreement with the experimental observations.

Thus, the experimental results confirm the theoretical prediction that olefin oxidation with H_2O_2 catalyzed by soluble Bi(III) salts occurs via two competitive reaction channels: the radical hydroperoxidation of the allylic C atom(s) and nonradical epoxidation of the C=C bond, and these channels are realized concurrently.

FINAL REMARKS

In this and previous[25] works, we have demonstrated for the first time that soluble Bi salts can exhibit catalytic activity toward the oxidation of hydrocarbons with H_2O_2. Such an oxidation of olefins occurs via two competitive channels: (i) nonradical epoxidation with possible subsequent hydrolysis of the epoxides to produce *trans* diols and (ii) radical hydroperoxidation of the allylic CH_2 groups to give alkenylhydroperoxides with involvement of the $HO^{\bullet}$ radical, which abstracts a hydrogen atom from the substrate molecule (Scheme 2). Theoretical (DFT) calculations predict that both epoxidation and hydroperoxidation pathways may be realized concurrently as a result of a rather small difference in the activation barriers.

The most plausible mechanism of epoxidation includes (i) the substitution of a water ligand for H_2O_2 in the initial aqua complex $[Bi(H_2O)_8]^{3+}$, (ii) the hydrolysis of the coordinated hydrogen peroxide, (iii) the one-step oxygen transfer through a direct attack of the olefin molecule at the unprotonated oxygen atom of the OOH^- ligand in $[Bi(H_2O)_5(OOH)]^{2+}$ via **TS1**, and (iv) the liberation of epoxide from the coordination sphere of bismuth (Schemes 5 and 6). Other concerted and stepwise mechanisms of epoxidation were found to be less favorable.

A preliminary experimental study of the cyclohexene, cyclooctene and 1-octene oxidation with the systems $Bi(NO_3)_3/H_2O_2/CH_3CN + H_2O$ and $BiCl_3/H_2O_2/CH_3CN + H_2O$ indicates the formation of both enol and epoxide/diol products, thus confirming the main conclusions of the theoretical calculations.

ASSOCIATED CONTENT

Supporting Information

The Supporting Information is available free of charge on the ACS Publications website at DOI: 10.1021/acscatal.5b00077.

Figures with curves of the products accumulation, tables with calculated total energies, enthalpies, entropies, and Gibbs free energies and Cartesian atomic coordinates for the equilibrium structures (PDF)

AUTHOR INFORMATION

Corresponding Author

*E-mail: max@mail.ist.utl.pt.

Notes

The authors declare no competing financial interest.

ACKNOWLEDGMENTS

The authors thank the Fundação para a Ciência e a Tecnologia (FCT), Portugal (Projects PTDC/QUI-QUI/119561/2010 and UID/QUI/00100/2013); the Russian Foundation for Basic Research (Grant 12-03-00084-a); and the "Science without Borders Program, Brazil−Russia", CAPES (Grant A017-2013) for support. B.G.M.R. is grateful to the Group V of Centro de Química Estrutural and FCT for fellowships BL/CQE-2012-026, BL/CQE-2013-010, and a Ph.D. fellowship of the CATSUS PhD program (SFRH/BD/52370/2013). M.L.K. thanks FCT and IST for a contract within the "FCT Investigator" program. G.B.S. expresses his gratitude to the FCT and Group V of Centro de Química Estrutural for making it possible for him to stay at the Instituto Superior Técnico, University of Lisbon, as invited Professor and to perform a part of the present work (all the funding for the invited scientist fellowship comes entirely from this Group).

REFERENCES

(1) (a) Shilov, A. E.; Shul'pin, G. B. *Chem. Rev.* **1997**, *97*, 2879−2932. (b) Weissermel, K.; Arpe, H.-J. *Industrial Organic Chemistry*; Wiley-VCH: New York, 2003; pp 1−491. (c) Schwesinger, J. W.; Bauer, T. Formation of C−O bonds by epoxidation of olefinic double bonds. In *Stereoselective Synthesis*; Helmchen, G., Hoffmann, R. W., Mulzer, J., Schaumann, E., Eds.; Houben Weyl Thieme: New York, 1995; Vol. *E21e*, pp 4599−4648. (d) Sheldon, R. A. Synthesis of oxiranes. In *Applied Homogeneous Catalysis with Organometallic*

DOI: 10.1021/acscatal.5b00077
ACS Catal. 2015, 5, 3823−3835

Compounds; Cornils, B., Herrmann, W. A., Eds.; Wiley-VCH: Weinheim, 1996; Vol. *1*, p 411−424. (e) Díaz-Requejo, M. M.; Pérez, P. J. *Chem. Rev.* **2008**, *108*, 3379−3394. (f) Crabtree, R. H. *Chem. Rev.* **1995**, *95*, 987−1007. (g) Jia, C.; Kitamura, T.; Fujiwara, Y. *Acc. Chem. Res.* **2001**, *34*, 633−639. (h) Labinger, J. A. *J. Mol. Catal. A: Chem.* **2004**, *220*, 27−35. (i) Conley, B. L.; Tenn, W. J., III; Young, K. J. H.; Ganesh, S. K.; Meier, S. K.; Ziatdinov, V. R.; Mironov, O.; Oxgaard, J.; Gonzales, J.; Goddard, W. A., III; Periana, R. A. *J. Mol. Catal. A: Chem.* **2006**, *251*, 8−23. (j) Muzart, J. J. *J. Mol. Catal. A: Chem.* **2007**, *276*, 62−72.

(2) (a) Lane, B. S.; Burgess, K. *Chem. Rev.* **2003**, *103*, 2457−2473. (b) Shul'pin, G. B. *Mini-Rev. Org. Chem.* **2009**, *6*, 95−104. (c) Grigoropoulou, G.; Clark, J. H.; Elings, J. A. *Green Chem.* **2003**, *5*, 1−7. (d) Brégeault, J.-M. *Dalton Trans.* **2003**, *17*, 3289−3302. (e) da Silva, J. A. L.; Fraústo da Silva, J. J. R.; Pombeiro, A. J. L. *Coord. Chem. Rev.* **2011**, *255*, 2232−2248. (f) Srour, H.; Le Maux, P.; Chevance, S.; Simonneaux, G. *Coord. Chem. Rev.* **2013**, *257*, 3030−3050. (g) Saisaha, P.; de Boerb, J. W.; Browne, W. R. *Chem. Soc. Rev.* **2013**, *42*, 2059−2074. (h) Talsi, E. P.; Bryliakov, K. P. *Coord. Chem. Rev.* **2012**, *256*, 1418−1434.

(3) (a) Huber, S.; Cokoja, M.; Kühn, F. E. *J. Organomet. Chem.* **2014**, *751*, 25−32. (b) Mayer, J. M. *Acc. Chem. Res.* **1998**, *31*, 441−450.

(4) (a) Thomas, J. M.; Raja, R.; Sankar, G.; Bell, R. G. *Acc. Chem. Res.* **2001**, *34*, 191−200. (b) Schuchardt, U.; Cardoso, D.; Sercheli, R.; Pereira, R.; da Cruz, R. S.; Guerreiro, M. C.; Mandelli, D.; Spinacé, E. V.; Pires, E. L. *Appl. Catal., A* **2001**, *211*, 1−17. (c) Tchenar, Y. N.; Choukchou-Braham, A.; Bachir, R. *Bull. Mater. Sci.* **2012**, *35*, 673−681. (d) Ciuffi, K. J.; de Faria, E. H.; Marçal, L.; Rocha, L. A.; Calefi, P. S.; Nassar, E. J.; Pepe, I.; da Rocha, Z. N.; Vicente, M. A.; Trujillano, R.; Gil, A.; Korili, S. A. *ACS Appl. Mater. Interfaces* **2012**, *4*, 2525−2533. (e) Ebadi, A.; Nikbakht, F. *React. Kinet., Mech. Catal.* **2011**, *104*, 37−47. (f) Kalam, A.; Rahman, L.; Kumashiro, M.; Ishihara, T. *Catal. Commun.* **2011**, *12*, 1198−1200. (g) Ricci, G. P.; Rocha, Z. N.; Nakagaki, S.; Castro, K. A. D. F.; Crotti, A. E. M.; Calefi, P. S.; Nassar, E. J.; Ciuffi, K. J. *Appl. Catal., A* **2010**, *389*, 147−154. (h) Borah, P.; Datta, A. *Appl. Catal., A* **2010**, *376*, 19−24. (i) Sadjadi, M. S.; Ebadi, A.; Zare, K. *React. Kinet., Mech. Catal.* **2010**, *99*, 119−124. (j) Aboelfetoh, E. F.; Pietschnig, R. *Catal. Lett.* **2009**, *127*, 83−94. (k) Mac Leod, T. C. O.; Guedes, D. F. C.; Lelo, M. R.; Rocha, R. A.; Caetano, B. L.; Ciuffi, K. J.; Assis, M. D. *J. Mol. Catal. A: Chem.* **2006**, *259*, 319−327. (l) Caetano, B. L.; Rocha, L. A.; Molina, E.; Rocha, Z. N.; Ricci, G.; Calefi, P. S.; de Lima, O. J.; Mello, C.; Nassar, E. J.; Ciuffi, K. J. *Appl. Catal., A* **2006**, *311*, 122−134. (m) Modén, B.; Zhan, B.−Z.; Dakka, J.; Santiesteban, J. G.; Iglesia, E. *J. Catal.* **2006**, *239*, 390−401. (n) Selvam, P.; Mohapatra, S. K. *J. Catal.* **2006**, *238*, 88−99. (o) Selvam, P.; Mohapatra, S. K. *J. Catal.* **2005**, *233*, 276−287. (p) Dapurkar, S. E.; Sakthivel, A.; Selvam, P. *J. Mol. Catal. A: Chem.* **2004**, *223*, 241−250. (q) Abbasov, A. A.; Zul'fugarova, S. Z.; Gasanova, L. M.; Nagiev, T. M. *Russ. J. Phys. Chem.* **2002**, *76*, 1591−1596. (r) Avdeev, M. V.; Bagrii, E. I.; Maravin, G. B.; Korolev, Y. M.; Borisov, R. S. *Petrol. Chem.* **2000**, *40*, 391−398. (s) Zahedi-Niaki, M. H.; Kapoor, M. P.; Kaliaguine, S. *J. Catal.* **1998**, *177*, 231−239. (t) Luna, F. J.; Ukawa, S. E.; Wallau, M.; Schuchardt, U. *J. Mol. Catal. A: Chem.* **1997**, *117*, 405−411. (u) Camblor, M. A.; Corma, A.; Perezpariente, J. *Zeolites* **1993**, *13*, 82−87. (v) Aboelfetoh, E. F.; Fechtelkord, M.; Pietschnig, R. *J. Mol. Catal. A: Chem.* **2010**, *318*, 51−59.

(5) (a) Mandelli, D.; do Amaral, A. C. N.; Kozlov, Y. N.; Shul'pina, L. S.; Bonon, A. J.; Carvalho, W. A.; Shul'pin, G. B. *Catal. Lett.* **2009**, *132*, 235−243. (b) Stoica, G.; Santiago, M.; Jacobs, P. A.; Perez-Ramirez, J.; Pescarmona, P. P. *Appl. Catal., A* **2009**, *371*, 43−53. (c) Pescarmona, P. P.; Jacobs, P. A. *Catal. Today* **2008**, *137*, 52−60. (d) Rinaldi, R.; Fujiwara, F. Y.; Schuchardt, U. *J. Catal.* **2007**, *245*, 456−465. (e) Uguina, M. A.; Delgado, J. A.; Rodriguez, A.; Carretero, J.; Gomez-Diaz, D. *J. Mol. Catal. A: Chem.* **2006**, *256*, 208−215. (f) Choudhary, V. R.; Patil, N. S.; Chaudhari, N. K.; Bhargava, S. K. *J. Mol. Catal. A: Chem.* **2005**, *227*, 217−222. (g) Pillai, U. R.; Sahle-Demessie, E. *Appl. Catal., A* **2004**, *261*, 69−76. (h) Fraile, J. M.; Garcia, J. I.; Marco, D.; Mayoral, J. A. *Appl. Catal., A* **2001**, *207*, 239−246. (i) Pescarmona, P. P.; Janssen, K. P. F.; Jacobs, P. A. *Chem. - Eur. J.* **2007**, *13*, 6562−6572. (j) Ionescu, R.; Pavel, O. D.; Bırjega, R.; Zavoianu, R.; Angelescu, E. *Catal. Lett.* **2010**, *134*, 309−317. (k) Sisodiya, S.; Shylesh, S.; Singh, A. P. *Catal. Commun.* **2011**, *12*, 629−633.

(6) (a) Asadullah, M.; Kitamura, T.; Fujiwara, Y. *Angew. Chem., Int. Ed.* **2000**, *39*, 2475. (b) Asadullah, M.; Kitamura, T.; Fujiwara, Y. *Appl. Organomet. Chem.* **1999**, *13*, 539−547. (c) Asadullah, M.; Kitamura, T.; Fujiwara, Y. *Catal. Lett.* **2000**, *69*, 37−41. (d) Asadullah, M.; Kitamura, T.; Fujiwara, Y. *J. Catal.* **2000**, *195*, 180−186. (e) Asadullah, M.; Taniguchi, Y.; Kitamura, T.; Fujiwara, Y. *Sekiyu Gakkaishi* **1998**, *41*, 236−239. (f) Asadullah, M.; Taniguchi, Y.; Kitamura, T.; Fujiwara, Y. *Appl. Organomet. Chem.* **1998**, *12*, 277−284.

(7) (a) Bian, X.; Gu, Q.; Shi, L.; Sun, Q. *Chin. J. Catal.* **2011**, *32*, 682−687. (b) Lu, X.; Lin, H.; Yuan, Y. *Chin. J. Catal.* **2010**, *31*, 1457−1464. (c) Gu, Q.; Han, D.; Shi, L.; Sun, Q. *J. Nat. Gas Chem.* **2012**, *21*, 452−458. (d) Li, Y. F. *Synlett* **2007**, *2007*, 2922−2923. (e) Choudhary, V. R.; Jha, R.; Jana, P. *Green Chem.* **2006**, *8*, 689−690. (f) Bonon, A. J.; Kozlov, Y. N.; Bahú, J. O.; Maciel Filho, R.; Mandelli, D.; Shul'pin, G. B. *J. Catal.* **2014**, *319*, 71−86.

(8) Mandelli, D.; Chiacchio, K. C.; Kozlov, Y. N.; Shul'pin, G. B. *Tetrahedron Lett.* **2008**, *49*, 6693−6697.

(9) Kuznetsov, M. L.; Teixeira, F. A.; Bokach, N. A.; Pombeiro, A. J. L.; Shul'pin, G. B. *J. Catal.* **2014**, *313*, 135−148.

(10) Rinaldi, R.; de Oliveira, H. F. N.; Schumann, H.; Schuchardt, U. *J. Mol. Catal. A: Chem.* **2009**, *307*, 1−8.

(11) Sever, R. R.; Root, T. W. *J. Phys. Chem. B* **2003**, *107*, 10521−10530.

(12) (a) Jiang, W.; Gorden, J. D.; Goldsmith, C. R. *Inorg. Chem.* **2012**, *51*, 2725−2727. (b) Jiang, W. C.; Gorden, J. D.; Goldsmith, C. R. *Inorg. Chem.* **2013**, *52*, 5814−5823.

(13) McKee, M. L.; Goldsmith, C. R. *Inorg. Chem.* **2014**, *53*, 318−326.

(14) (a) Hua, R. *Curr. Org. Synth.* **2008**, *5*, 1−27. (b) Ollevier, T. *Org. Biomol. Chem.* **2013**, *11*, 2740−2755.

(15) (a) Wang, H.-L.; Li, R.; Zheng, Y.-F.; Chen, H.-N.; Jin, J.; Wang, F.-S.; Ma, J.-T. *Helv. Chim. Acta* **2007**, *90*, 1837−1847. (b) Qian, G.; Ji, D.; Lu, G.; Zhao, R.; Qi, Y.; Suo, J. *J. Catal.* **2005**, *232*, 378−385. (c) Qian, G.; Lu, G.; Ji, D.; Zhao, R.; Qi, Y.; Suo, J. *Chem. Lett.* **2005**, *34*, 162−163.

(16) Dumitriu, D.; Barjega, R.; Frunza, L.; Macovei, D.; Hu, T.; Xie, Y.; Parvulescu, V. I.; Kaliaguine, S. *J. Catal.* **2003**, *219*, 337−351.

(17) (a) Bonvin, Y.; Callens, E.; Larrosa, I.; Henderson, D. A.; Oldham, J.; Burton, A. J.; Barrett, A. G. M. *Org. Lett.* **2005**, *7*, 4549−4552. (b) Callens, E.; Burton, A. J.; White, A. J. P.; Barrett, A. G. M. *Tetrahedron Lett.* **2008**, *49*, 3709−3712. (c) Salvador, J. A. R.; Silvestre, S. M. *Tetrahedron Lett.* **2005**, *46*, 2581−2584.

(18) Banik, B. K.; Venkatraman, M. S.; Mukhopadhyay, C.; Becker, F. F. *Tetrahedron Lett.* **1998**, *39*, 7247−7250.

(19) Pang, Y.; Chen, X.; Xu, C.; Lei, Y.; Wei, K. *ChemCatChem* **2014**, *6*, 876−884.

(20) Zhai, Z.; Getsoian, A. "B."; Bell, A. T. *J. Catal.* **2013**, *308*, 25−36.

(21) (a) Franzke, T.; Rosowski, F.; Muhler, M. *Chem. Ing. Tech.* **2011**, *83*, 1705−1710. (b) Goddard, W. A., III; Duin, A.; Chenoweth, K.; Cheng, M.; Pudar, S.; Oxgaard, J.; Merinov, B.; Jang, Y. H.; Persson, P. *Top. Catal.* **2006**, *38*, 93−103. (c) Allison, J. N.; Goddard, W. A., III *ACS Symp. Ser.* **1985**, *279*, 23−26. (d) Obana, Y.; Yashiki, K.; Ito, M.; Nishiguchi, H.; Ishihara, T.; Takita, Y. *J. Jpn. Pet. Inst.* **2003**, *46*, 53−61. (e) Tsunoda, T.; Hayakawa, T.; Kameyama, T.; Fukudat, K.; Takehira, K. *J. Chem. Soc., Faraday Trans.* **1995**, *91*, 1117−1124. (f) Ono, T.; Ogata, N.; Kuczkowski, R. L. *J. Catal.* **1998**, *175*, 185−193. (g) Moens, L.; Ruiz, P.; Delmon, B.; Devillers, M. *Appl. Catal., A* **2003**, *249*, 365−374.

(22) Hunger, M.; Limberg, C.; Kaifer, E.; Rutsch, P. *J. Organomet. Chem.* **2002**, *641*, 9−14.

(23) Bienati, M.; Bonacic-Koutecky, V.; Fantucci, P. *J. Phys. Chem. A* **2000**, *104*, 6983−6992.

DOI: 10.1021/acscatal.5b00077
ACS Catal. 2015, 5, 3823−3835

(24) (a) Fielicke, A.; Rademann, K. *J. Phys. Chem. A* **2000**, *104*, 6979−6982. (b) Kinne, M.; Heidenreich, A.; Rademann, K. *Angew. Chem., Int. Ed.* **1998**, *37*, 2509−2511.
(25) Rocha, B. G. M.; Kuznetsov, M. L.; Kozlov, Y. N.; Pombeiro, A. J. L.; Shul'pin, G. B. *Catal. Sci. Technol.* **2015**, *5*, 2174−2187.
(26) (a) Kuznetsov, M. L.; Kozlov, Y. N.; Mandelli, D.; Pombeiro, A. J. L.; Shul'pin, G. B. *Inorg. Chem.* **2011**, *50*, 3996−4005. (b) Novikov, A. S.; Kuznetsov, M. L.; Pombeiro, A. J. L.; Bokach, N. A.; Shul'pin, G. B. *ACS Catal.* **2013**, *3*, 1195−1208.
(27) (a) Becke, A. D. *J. Chem. Phys.* **1993**, *98*, 5648−5652. (b) Lee, C.; Yang, W.; Parr, R. G. *Phys. Rev. B: Condens. Matter Mater. Phys.* **1988**, *37*, 785−789.
(28) Frisch, M. J.; Trucks, G. W.; Schlegel, H. B.; Scuseria, G. E.; Robb, M. A.; Cheeseman, J. R.; Scalmani, G.; Barone, V.; Mennucci, B.; Petersson, G. A.; Nakatsuji, H.; Caricato, M.; Li, X.; Hratchian, H. P.; Izmaylov, A. F.; Bloino, J.; Zheng, G.; Sonnenberg, J. L.; Hada, M.; Ehara, M.; Toyota, K.; Fukuda, R.; Hasegawa, J.; Ishida, M.; Nakajima, T.; Honda, Y.; Kitao, O.; Nakai, H.; Vreven, T.; Montgomery, J. A., Jr.; Peralta, J. E.; Ogliaro, F.; Bearpark, M.; Heyd, J. J.; Brothers, E.; Kudin, K. N.; Staroverov, V. N.; Kobayashi, R.; Normand, J.; Raghavachari, K.; Rendell, A.; Burant, J. C.; Iyengar, S. S.; Tomasi, J.; Cossi, M.; Rega, N.; Millam, J. M.; Klene, M.; Knox, J. E.; Cross, J. B.; Bakken, V.; Adamo, C.; Jaramillo, J.; Gomperts, R.; Stratmann, R. E.; Yazyev, O.; Austin, A. J.; Cammi, R.; Pomelli, C.; Ochterski, J. W.; Martin, R. L.; Morokuma, K.; Zakrzewski, V. G.; Voth, G. A.; Salvador, P.; Dannenberg, J. J.; Dapprich, S.; Daniels, A. D.; Farkas, O.; Foresman, J. B.; Ortiz, J. V.; Cioslowski, J.; Fox, D. J. *Gaussian 09, Revision A.01*, Gaussian, Inc.: Wallingford, CT, 2009.
(29) Kuchle, W.; Dolg, M.; Stoll, H.; Preuss, H. *Mol. Phys.* **1991**, *74*, 1245−1263.
(30) (a) McLean, A. D.; Chandler, G. S. *J. Chem. Phys.* **1980**, *72*, 5639−5648. (b) Krishnan, R.; Binkley, J. S.; Seeger, R.; Pople, J. A. *J. Chem. Phys.* **1980**, *72*, 650−654. (c) Wachters, A. J. H. *J. Chem. Phys.* **1970**, *52*, 1033−1036. (d) Hay, P. J. *J. Chem. Phys.* **1977**, *66*, 4377−4384.
(31) Gonzalez, C.; Schlegel, H. B. *J. Chem. Phys.* **1991**, *95*, 5853−5860.
(32) Barone, V.; Cossi, M. *J. Phys. Chem. A* **1998**, *102*, 1995−2001.
(33) Frisch, M. J.; Trucks, G. W.; Schlegel, H. B.; Scuseria, G. E.; Robb, M. A.; Cheeseman, J. R.; Montgomery, J. A.; Vreven, J. T. ; Kudin, K. N.; Burant, J. C.; Millam, J. M.; Iyengar, S. S.; Tomasi, J.; Barone, V.; Mennucci, B.; Cossi, M.; Scalmani, G.; Rega, N.; Petersson, G. A.; Nakatsuji, H.; Hada, M.; Ehara, M.; Toyota, K.; Fukuda, R.; Hasegawa, J.; Ishida, M.; Nakajima, T.; Honda, Y.; Kitao, O.; Nakai, H.; Klene, M.; Li, X.; Knox, J. E.; Hratchian, H. P.; Cross, J. B.; Bakken, V.; Adamo, C.; Jaramillo, J.; Gomperts, R.; Stratmann, R. E.; Yazyev, O.; Austin, A. J.; Cammi, R.; Pomelli, C.; Ochterski, J. W.; Ayala, P. Y.; Morokuma, K.; Voth, G. A.; Salvador, P.; Dannenberg, J. J.; Zakrzewski, V. G.; Dapprich, S.; Daniels, A. D.; Strain, M. C.; Farkas, O.; Malick, D. K.; Rabuck, A. D.; Raghavachari, K.; Foresman, J. B.; Ortiz, J. V.; Cui, Q.; Baboul, A. G.; Clifford, S.; Cioslowski, J.; Stefanov, B. B.; Liu, G.; Liashenko, A.; Piskorz, P.; Komaromi, I.; Martin, R. L.; Fox, D. J.; Keith, T.; Al-Laham, M. A.; Peng, C. Y.; Nanayakkara, A.; Challacombe, M.; Gill, P. M. W.; Johnson, B.; Chen, W.; Wong, M. W.; Gonzalez, C.; Pople, J. A. *Gaussian 03, revision B.05*; Gaussian, Inc.: Wallingford, CT, 2004.
(34) (a) Barone, V.; Cossi, M.; Tomasi, J. *J. Chem. Phys.* **1997**, *107*, 3210−3221. (b) Perdew, J. P.; Burke, K.; Ernzerhof, M. *Phys. Rev. Lett.* **1996**, *77*, 3865−3868. (c) Perdew, J. P.; Burke, K.; Ernzerhof, M. *Phys. Rev. Lett.* **1997**, *78*, 1396. (d) Adamo, C.; Barone, V. *J. Chem. Phys.* **1999**, *110*, 6158−6169.
(35) (a) Wertz, D. H. *J. Am. Chem. Soc.* **1980**, *102*, 5316−5322. (b) Cooper, J.; Ziegler, T. *Inorg. Chem.* **2002**, *41*, 6614−6622.
(36) Bader, R. F. W. *Atoms in Molecules: A Quantum Theory*; Oxford University Press: Oxford, 1994; pp 1−458.
(37) Keith, T. A. *AIMAll (Version 14.10.27)*; TK Gristmill Software: Overland Park KS, USA, 2014; (aim.tkgristmill.com).
(38) Wiberg, K. B. *Tetrahedron* **1968**, *24*, 1083−1096.
(39) Reed, A. E.; Curtiss, L. A.; Weinhold, F. *Chem. Rev.* **1988**, *88*, 899−926.
(40) (a) Moyano, A.; Pericàs, M. A.; Valentí, E. *J. Org. Chem.* **1989**, *54*, 573−582. (b) Lecea, B.; Arrieta, A.; Roa, G.; Ugalde, J. M.; Cossío, F. P. *J. Am. Chem. Soc.* **1994**, *116*, 9613−9619. (c) Morao, I.; Lecea, B.; Cossío, F. P. *J. Org. Chem.* **1997**, *62*, 7033−7036. (d) Cossío, F. P.; Morao, I.; Jiao, H.; Schleyer, P. v. R. *J. Am. Chem. Soc.* **1999**, *121*, 6737−6746.
(41) (a) Shul'pin, G. B. *J. Mol. Catal. A: Chem.* **2002**, *189*, 39−66. (b) Shul'pin, G. B. *Org. Biomol. Chem.* **2010**, *8*, 4217−4228. (c) Shul'pin, G. B. *Dalton Trans.* **2013**, *42*, 12794−12818.
(42) Sharpless, K. B.; Townsend, J. M.; Williams, D. R. *J. Am. Chem. Soc.* **1972**, *94*, 295−296.
(43) (a) Karlsen, E.; Schoffel, K. *Catal. Today* **1996**, *32*, 107−114. (b) Tantanak, D.; Vincent, M. A.; Hillier, I. H. *Chem. Commun.* **1998**, 1031−1032. (c) Sever, R. R.; Root, T. W. *J. Phys. Chem. B* **2003**, *107*, 4090−4099.
(44) (a) Thiel, W. R. *J. Mol. Catal. A: Chem.* **1997**, *117*, 449−454. (b) Thiel, W. R.; Eppinger, J. *Chem. - Eur. J.* **1997**, *3*, 696−705.
(45) Mimoun, H.; Seree de Roch, I.; Sajus, L. *Tetrahedron* **1970**, *26*, 37−50.
(46) (a) Veiros, L. F.; Prazeres, Â.; Costa, P. J.; Romão, C. C.; Kühn, F. E.; Calhorda, M. J. *Dalton Trans.* **2006**, 1383−1389. (b) Costa, P. J.; Calhorda, M. J.; Kühn, F. E. *Organometallics* **2010**, *29*, 303−311.
(47) (a) Näslund, J.; Persson, I.; Sandstrom, M. *Inorg. Chem.* **2000**, *39*, 4012−4021. (b) Durdagi, S.; Hofer, T. S.; Randolf, B. R.; Rode, B. M. *Chem. Phys. Lett.* **2005**, *406*, 20−23. (c) Khan, A.; Weiss, A. K. H.; Uddin, R.; Randolf, B. R.; Rode, B. M.; Hofer, T. S. *J. Phys. Chem. A* **2012**, *116*, 8008−8014.
(48) Sun, H.; Zhang, L.; Szeto, K.-Y. Bismuth in medicine. In *Metal Ions in Biological Systems*; Sigel, A., Sigel, H., Eds.; FontisMedia S.A.: Lausanne, 2004, Vol. *41*, pp 333−378.
(49) (a) Wulfsberg, G. *Principles of Descriptive Inorganic Chemistry*; University Science Books: Sausalito, 1991; pp 1−467. (b) Kobayashi, S.; Ueno, M.; Kitanosono, T. Bismuth catalysts in aqueous media. In *Bismuth-Mediated Organic Reactions*; Ollevier, T., Ed.; Springer: Heidelberg, 2012; pp 1−18.
(50) (a) Anjaneyulu, O.; Maddileti, D.; Swamy, K. C. K. *Dalton Trans.* **2012**, *41*, 1004−1012. (b) Sukhov, B. G.; Mukha, S. A.; Antipova, I. A.; Medvedeva, S. A.; Larina, L. I.; Chipanina, N. N.; Kazheva, O. N.; Shilov, G. V.; Dyachenko, O. A.; Trofimov, B. A. *ARKIVOC* **2008**, *2008*, 139−149. (c) Rivenet, M.; Roussel, P.; Abraham, F. *J. Solid State Chem.* **2008**, *181*, 2586−2590. (d) Sun, R.-Z.; Guo, Y.-C.; Liu, W.-M.; Chen, S.-Y.; Feng, Y.-Q. *Chin. J. Struct. Chem.* **2012**, *31*, 655−660.
(51) Deubel, D. V.; Sundermeyer, J.; Frenking, G. *J. Am. Chem. Soc.* **2000**, *122*, 10101−10108.
(52) Clegg, W.; Errington, R. J.; Fisher, G. A.; Hockless, D. C. R.; Norman, N. C.; Orpen, A. G.; Stratford, S. E. *J. Chem. Soc., Dalton Trans.* **1992**, 1967−1974.
(53) The CPCM method and the model with one or two explicit solvent molecules in the second coordination sphere do not allow the correct calculations of the energies for reactions in which the number of the species with the same charge is not preserved, for example, hydrolysis.[26a] Hence, also taking into account that the experimental pK_{a2} value is unknown for the Bi(III) species, the energies of formation of **9** or **11** from **3** were not estimated. However, considering that the ΔG_s of the hydrolysis of **2** is positive,[25] the hydrolysis of complex **3** with a lower overall charge should be even more endoergonic.
(54) Kuznetsov, M. L.; Pessoa, J. C. *Dalton Trans.* **2009**, 5460−5468.

DOI: 10.1021/acscatal.5b00077
ACS Catal. 2015, 5, 3823−3835